

# FINAL REPORT

## **Investigation of nocturnal surface wind bias by the Weather Research and Forecasting (WRF)/ Advanced Research WRF (ARW) meteorological model for the Second Texas Air Quality Study (TexAQS-II) in 2006**

March 15, 2012

*Submitted by*  
Air Resources Laboratory  
National Oceanic and Atmospheric Administration  
U.S. Department of Commerce  
SSMC3, Rm 3316 (R/ARL)  
1315 East West Highway  
Silver Spring, Maryland 20910-3282

*Principal Investigator*  
Pius Lee

*Investigators*  
Hyun-Cheol Kim, Fantine Ngan

*Prepared for*  
Texas Commission on Environmental Quality

Project manager: Khalid Al-Wali  
Air Quality Division  
[Khalid.Al-Wali@tceq.texas.gov](mailto:Khalid.Al-Wali@tceq.texas.gov)

## PROJECT SUMMARY

This project studies the nocturnal surface wind bias in the WRF-ARW model for the TexAQS-II period. Daytime wind is responsible for the accuracy of capturing the local maxima of concentrations in air quality modeling while nighttime wind prediction is important for capturing the transport of precursors that initiate the photochemistry for the following day. We intend to analyze the characteristics of the nocturnal wind bias problem through three prospective: (1) pin point when and where the bias occurs and its dependence on synoptic weather patterns, (2) develop a conceptual model of the nocturnal boundary layer winds from observations and modeling studies, and (3) investigate the components and parameterization of the momentum and thermodynamic equations controlling evolution of the nocturnal boundary layer that may be responsible for the near surface wind bias.

A 37-day simulation was done for a period of TexAQS-II, May 28 – July 3, 2006 using the WRF-ARW model. The result shows that model tends to increase the wind speed, especially in the coastal region such as the Houston-Galveston-Brazoria (HGB) area, at the evening hours; whereas the observations show the opposite. The evening wind bias usually starts around 19 CST when sun goes down leading to the growth of nocturnal boundary layer. The period June 4 – 12 lies between two frontal passages over HGB repeatedly had the wind bias problem at the sunset hour. During that period, a high pressure system centered at Louisiana/Mississippi/Arkansas area caused the southeastern Texas under the influence of easterly/southeasterly flow in the low troposphere. The weather condition was favorable to sea breeze development, which brings southerly to southwesterly onshore flow in the near surface levels.

The comparison with the wind tower measurement at UH Coastal Center site for the same periods showed that the evening wind bias problem seemed to be confined very close to the surface, where the wind direction was mostly southerly/southwesterly. Sensible heat flux was over-predicted during nighttime causing warm bias for 2-m temperature and indicating possibly too much downward transport and/or too large downward incident long wave radiation. The wind profiler analysis showed the sea breeze driven nocturnal low-level jet was favorably present at around 300 m height on the day with evening wind bias. Southerly to southwesterly was dominant within the nocturnal boundary layer. Another wind maximum could be seen at the higher level at around 1.5 – 2 km associated with high pressure system centered in the southeastern states. The hodograph derived from both model and observations in the hundreds meters level of height (less than 300 m) demonstrated nice forward turning over time. However, for the hodograph corresponding to the surface winds, model experienced forward oscillation contrary with observation had backward turning.

Table of Contents

<b>1. Introduction</b> .....	<b>5</b>
<b>2. Overview of wind Bias problem</b> .....	<b>6</b>
<b>3. The Use of model data and observations</b> .....	<b>7</b>
a. Model configuration .....	7
b. Observations for analysis.....	9
<b>4. Quality Assurance/Quality Control Procedures</b> .....	<b>9</b>
<b>5. Results and discussions</b> .....	<b>10</b>
a. Identification of wind bias period.....	10
b. Characteristics of weather patterns.....	14
c. Comparison at UH Coastal Center .....	15
d. Analysis of wind profiler paring with surface observations .....	17
<b>6. Conclusive Remarks and Future Work</b> .....	<b>21</b>
<b>7. Reference</b> .....	<b>23</b>
<b>Appendix A</b> .....	<b>25</b>
<b>Appendix B</b> .....	<b>26</b>
<b>Appendix C</b> .....	<b>26</b>

LIST OF FIGURES

FIG. 1. WRF domains used for model simulations in three different spatial resolutions: 36-km (NA36), 12-km (SUS12) and 4-km (TX04). ..... 8

FIG. 2. CAMS stations map color coded with 5-selected region. The number of station in each region is printed next to the sector's label. .... 9

FIG. 3 Time series of 10-m wind speed bias (model – CAMS observations) averaged for the TX04 domain. Black line is observations while red line is model result. .... 11

FIG. 4 Spatial distribution of bias for 10-m wind speed for daytime hours (left) and nighttime hours (right). .... 11

FIG. 5 Time series of 10-m wind speed predicted by WRF (red line) and CAMS surface observations (black line) averaged for (a) HGB and (b) DFW regions. Shaded areas are rainy days and purple arrows indicate frontal passage. Black line is observations while red line is model result. .... 12

FIG. 6 Diurnal variation of HGB (top) and DFW (bottom) regional average surface wind speed for period June 4 – 12 (dark color) and June 26 – July 3 (light color). .... 13

FIG. 7 Composite weather chart for large wind bias period (6/4 – 6/12) and less wind bias period (6/26 – 7/3) at the surface (top panel) and on 850 hPa level (bottom panel). .... 14

FIG. 8 Time series of 10-m wind speed (top) and wind direction (bottom) at UHCC station for large wind bias period (6/4 – 6/12, left) and small wind bias period (6/26 – 7/3, right). Gray color is observations while red color is model result. .... 15

FIG. 9 Time series comparison of 43-m height observed wind (gray color) with 1<sup>st</sup> layer model wind (~16.9 m, pink line) and 2<sup>nd</sup> layer model wind (~59.4 m, red line) for large wind bias period at UHCC station. .... 16

FIG. 10 Time series of 2-m temperature (top), sensible heat flux (middle) and latent heat flux (bottom) at UHCC for large wind bias period (6/4 – 6/12, left) and small wind bias period (6/26 – 7/3, right). .... 16

FIG. 11 Time series of wind speed of model and CAMS site C35. Observed is in black while model values are in red (10 m), pink (1<sup>st</sup> layer) and orange (2<sup>nd</sup> layer). .... 18

FIG. 12 Wind profiler plot at La Porte site for June 10<sup>th</sup> and 11<sup>th</sup>. Top panel: model and bottom panel: observation. .... 18

FIG. 13 Wind profiler plot at La Porte site for June 10<sup>th</sup> and 11<sup>th</sup>. Top panel: model and bottom panel: observation. .... 19

FIG. 14 Hodograph at the surface (CAMS site C35) and La Porte site at 53m and 350m above ground level on 6/10 12 CST – 6/11 17 CST. The color of dot represents time of the hour. .... 20

LIST OF TABLES

TABLE 1. Model configurations used in this study. .... 8

## 1. Introduction

Accurate simulation of surface winds by a mesoscale model is critically important for the accurate understanding of the role of different emission sources contributing to high air pollution events in a region. Air quality episodes often arise as a result of active photochemical reactions during the daytime, whereas the nocturnal transport processes determine the morning ozone and the precursor concentrations that initiate photochemistry for the following day. Banta et al. (2011) investigated the dependence of ozone peak on environmental factors for two TexAQS campaigns showed that wind speed is the most sensitive meteorological variable that strongly associated with maximum ozone. Over-prediction of wind speed input for ozone simulations resulted in misplacement of ozone plume and its magnitude (Ngan et al. 2012).

The Weather Research and Forecasting (WRF) model (Shamarock et al. 2008) and its predecessor – the National Center for Atmospheric Research (NCAR) / Pennsylvania State University (PSU) Fifth Generation Mesoscale Model (MM5) (Grell et al. 1994) – frequently overestimate surface wind speeds during nighttime hours in the states adjacent to the Gulf of Mexico (e.g., Byun et al., 2008 and Lee et al., 2010), in the central United States (Zhang and Zheng, 2004), and coastal city of Spain (Chen et al., 2012). The wind errors can lead to inaccurate prediction of precursor conditions affecting the evolution of air pollution events in the metropolitan. With the help of data assimilation technique in current meteorological model, nocturnal wind bias problem can be minimized in the retrospective simulations for air quality modeling (Gilliam and Pleim 2010, Otte 2008 and Ngan et al. 2012). However, over-prediction of wind speed jeopardizes accuracy of air quality forecast when surface observations are not available in real-time for data assimilation. Similar behavior was documented with the University of Houston MM5 predictions used for the Eastern Texas Air Quality (ETAQ) forecasting system (Byun et al., 2007). The days with large over-prediction of nighttime winds often coincided with fair-weather days with dominantly southerly to southwesterly winds.

The goal of this project is to understand the characteristics of the nocturnal wind bias problem in the WRF-ARW meteorological model through three prospective: (1) pin point when and where the bias occurs and its dependence on synoptic weather patterns, (2) develop a conceptual model of the nocturnal boundary layer winds from observations and modeling studies, and (3) investigate the components of the momentum and thermodynamic equations controlling evolution of the nocturnal boundary layer pointing to possible causes of the surface wind bias.

Attribution of such frequent and possible systematic model high wind-speed biases will potentially enable a local health agency or air quality forecaster to rectify the simulation related deficiency. One can identify when and how such inaccurate meteorological simulations may affect predicted air pollution precursor concentrations. By generalizing such deficient meteorological fields one may give possible remedial guidance to the forecaster. Furthermore investigation of the components of the momentum and thermodynamic equations that control evolution of the nocturnal boundary layer can lead to model parameterization improvement for the WRF model.

## 2. Overview of wind Bias problem

There may be various reasons why meteorological models exhibit such deficiencies as nocturnal wind speed overestimation. Zhang and Zheng (2004) analyzed the relation of diurnal cycle of surface wind speed and temperature and their sensitivity to the PBL parameterizations. Their results indicate that even with well simulated cycle of surface temperature (and the thermal structures above) the reproduction of the diurnal cycles of surface wind depends on proper parameterization of physical process – strong vertical coupling in daytime and vertically decoupling at night. In the presence of low-level jet in the top of nocturnal boundary layer, excessive downward transport may have caused the over-prediction of wind.

Lee et al (2011) attempted to improve WRF model simulations for Southeastern Texas by introducing the urban parameterization in the Noah land surface model (LSM). It showed better performance in the comparisons of PBL height and near surface temperature than with the original Noah LSM but its impact on the wind field was relatively small. By showing the overestimation of surface wind speed and underestimation of wind around 300 hPa above ground, as well as the over-prediction of sensible heat flux and nighttime PBL height, they concluded that enhanced momentum was transferred downward through an excessive vertical mixing, resulting the wind speed bias near the surface.

In the coastal environment such as the HGB area, sea breeze oscillation is frequently present during the summer time. The local circulation is the combination of larger-scale synoptic gradient wind and diurnal varying sea breeze component (Banta et al. 2005). Nielsen-Gammon (2002) reported modeling studies of nocturnal low-level jet (southwesterly) formed in the HGB area in a weather condition dominated by a strong subtropical high system centered at the East coast of the Nation. Tucker et al. (2010) identified two flow regimes featuring different LLJ characteristics and their relationship with ozone. They pointed out similar surface wind variation during nighttime accompanied with distinguishable nocturnal boundary layer wind structures. One of the vertical profiles mentioned in the study was the LLJ core at around 300 m height and with wind speed of 5 m/s co-existed with stagnant zone at around 500 – 700 m. The wind speed increased again with height and reached around 15 m/s above 2km. Another type was a simpler wind vertical structure – the jet core present at around 1 km, with wind speed around 15 m/s in southerly to southwesterly wind direction.

The conceptual model of nocturnal oscillation proposed by Blackadar (1957) often used to explain development of low-level wind maximum at night, the so-called nocturnal low-level jet (LLJ). The theory suggests that nocturnal winds above the stable boundary layer are subject to oscillation around the geostrophic wind with a period of a half-pendulum day, which is about 12-hours in southern Texas. It assumes that inertial oscillation starts as turbulent fluxes die away after sunset. However the Blackadar model cannot be directly applied to explain winds within the nocturnal boundary layer. Andreas et al. (2000) successfully applied a similar two-layer model to describe observed nocturnal wind structure observed at the Ice Station Weddell (ISW) in Antarctica. They showed that wind in the boundary layer exhibited a similar inertial oscillation, but around the equilibrium wind determined by the steady state solution accounted for surface drag (e.g., Byun and Arya, 1986). Van de Wiel et al. (2010) extended the concept of

nocturnal inertial oscillations in Blackadar (1957) by introducing frictional effect within nocturnal boundary layer. They showed that the surface winds are subject to the backward inertial oscillations which appear to be present in observations (sounding at Cabauw Observatory in Netherlands) as well. Thus the forward inertial oscillation may be responsible for increasing of wind speed in the LLJ while the backward oscillation is associated with the weakening of LLJ.

### **3. The Use of model data and observations**

#### *a. Model configuration*

The modeling domain structure consists of nested domains of different resolutions: a coarse grid domain (36-km cell size, named as ‘NA36’) that covers the continental United States, a regional domain (12-km cell size, named as ‘SUS12’) over the Texas and neighboring the Gulf of Mexico areas, and a fine domain (4-km cell size, named as ‘TX04’) covering the Eastern Texas area (FIG. 1). They were defined on a Lambert Conformal mapping projection with the first true latitude (alpha) at 33°N, second true latitude (beta) at 45°N, central longitude (gamma) at 97°W, and the projection origin at (97°W, 40°N). Following the TCEQ’s SIP model set up, we used 43 vertical sigma layers extending the surface to the 50-hPa level, with higher resolution near the ground to better understand the atmospheric structure in the lower boundary layer. The first half sigma level is around 17 m above ground level.

WRF version 3.2 was used to simulate weather condition of time period between May 28<sup>th</sup> and July 3<sup>rd</sup>, 2006 (totaled 37 days). The initial and boundary conditions for WRF originate from the National Centers for Environmental Prediction (NCEP) North American Mesoscale (NAM) 3 hourly analyses while the sea surface temperature (SST) was updated daily by the NCEP real-time global sea surface temperature analysis in 0.5 deg grid spacing. NA36 and SUS12 domains were run with 2-way nesting with 3D grid nudging. The TX04 domain was initialized by the nest-down of SUS12 result. Considering the scope of this study for investigating the nighttime wind bias, the use of surface analysis and observational nudging were not used in the simulation. But grid nudging was operated in TX04 domain as used in the coarse domains. The physics options and model configuration used in the WRF simulation are listed in TABLE 1.

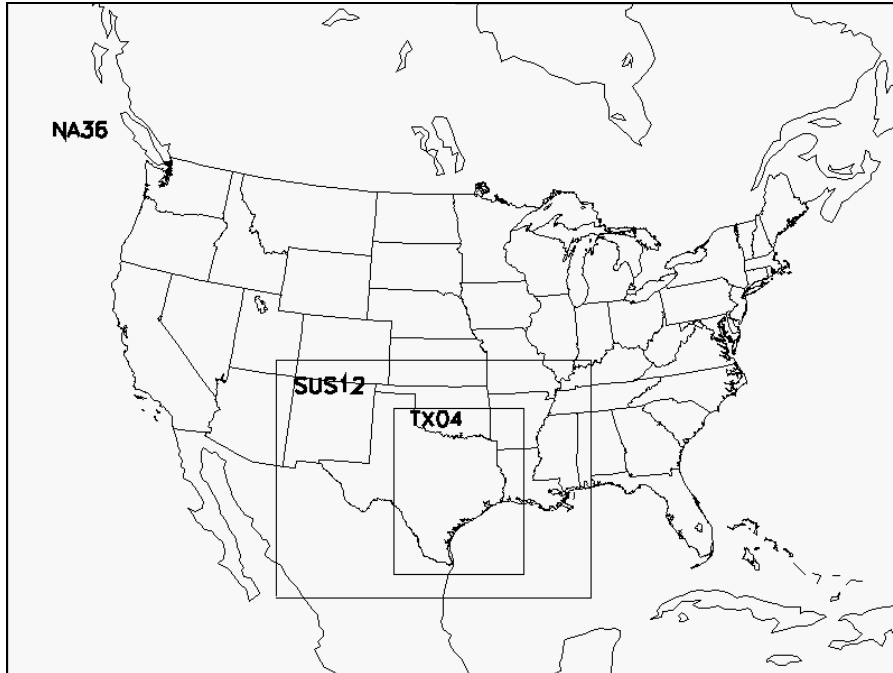


FIG. 1. WRF domains used for model simulations in three different spatial resolutions: 36-km (NA36), 12-km (SUS12) and 4-km (TX04).

TABLE 1. Model configurations used in this study.

Domain name	NA36	SUS12	TX04
Resolution	36 km	12 km	4 km
Domain coverage	Continental US	Texas & adjoining states	Eastern Texas
Horizontal grid	162 x 128	174 x 138	216 x 288
Initialization	NAM + NCEP daily SST Run in 2-way nesting		Nest-down of SUS12
Microphysics	WSM5 <sup>a</sup>		WSM6 <sup>b</sup>
Cloud scheme	KF <sup>c</sup>		None
Radiation scheme	RRTM <sup>d</sup> for longwave radiation MM5 (Dudhia) <sup>e</sup> for shortwave radiation		
PBL scheme	YSU <sup>f</sup> scheme		
Land surface model	5-layer slab model <sup>g</sup>		
Nudging	3D grid nudging (no nudging of mass fields within PBL)		

<sup>a</sup> WRF Single-Moment 5-class (Hong et al., 2004). <sup>b</sup> WRF Single-Moment 6-class (Hong and Lim, 2006). <sup>c</sup> Kain and Fritsch scheme (Kain, 2004). <sup>d</sup> Rapid Radiative Transfer Model scheme (Mlawer et al. 1997). <sup>e</sup> Dudhia (1989). <sup>f</sup> Yonsei University scheme (Hong et al., 2006). <sup>g</sup> 5-layer soil temperature model (Grell et al., 1994).

*b. Observations for analysis*

The evaluation of model results was done against Continuous Air Monitoring Site (CAMS) data (FIG. 2). To understand the spatial distribution of nocturnal wind biases, the CAMS stations were grouped geographically into 5 regions. They are Houston-Galveston-Brazoria region (HGB), Dallas-Fort Bend region (DFW), Beaumont region (BEA), Corpus Christi region (CCA) and Austin-San Antonio region (ASA). Among these regions, HGB, BEA and CCA are considered as coastal environment while DFW and ASA are representing inland characteristics. Within the HGB region, a wind profiler operated by Cooperative Agency Profilers (CAP, <https://madis-data.noaa.gov/cap/>) is available at La Porte (LPTTX) which is paired with CAMS site C35. The UH Coastal Center (hereafter UHCC) is a station operated by University of Houston to measure meteorological parameters including temperature, wind, precipitation and fluxes. It locates at southeast of the Houston metropolitan area and about 15 miles away from the Gulf of Mexico. Sampling was done every minute for meteorological variables but every 10 minutes for fluxes. There is a tower providing wind measurement at 2 m, 10 m, 20 m and 43 m above ground level.

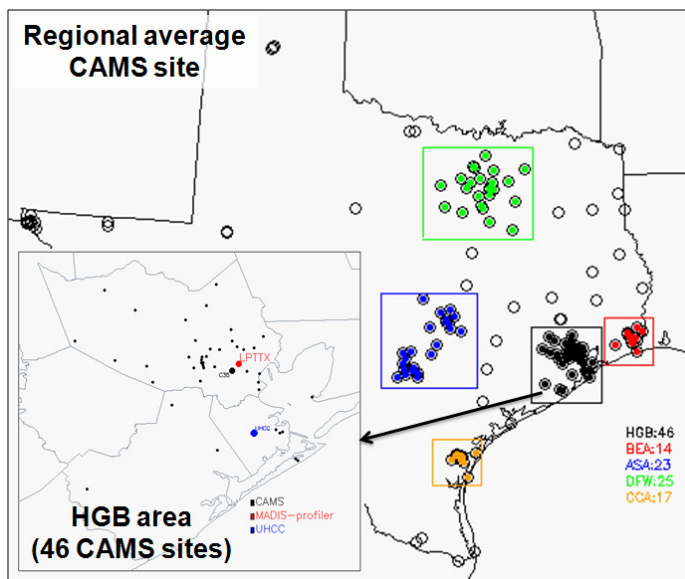


**FIG. 2.** CAMS stations map color coded with 5-selected region. The number of station in each region is printed next to the sector's label.

#### **4. Quality Assurance/Quality Control Procedures**

This project was established upon the QA Categories III which is listed in the QAPP document submitted in June 2011. Modeling domains shown in the previous section was identical as TCEQ's WRF model configuration. The simulation used the "namelist.wps" and "namelist.input" files (control file for running WPS and WRF, respectively) downloaded from TCEQ. Emails were exchanged between ARL and TCEQ to confirm that the simulation run in ARL machine following the operation done in TCEQ. The WRF run encountered no error during the simulation. The CAMS stations data in METSTAT ASCII format was downloaded from TCEQ ftp site. An IDL subroutine was programmed to compute the statistics and analysis shown in the following sections.

The UH Coastal Center data were obtained from UH IMAQS (Institute for Multi-dimensional Air Quality Studies) measurement team through the personal contact with Prof. Bernhard Rappenglueck, who is the one of the co-PI of the Houston-Network of Environment Towers (H-NET) project (<http://www.hnet.uh.edu/about.php>). The data is archived in ASCII format. An IDL program was made to read the files and extracted the corresponding model output for the comparisons. There is no missing data throughout the study period. For the wind profiler data, it was collected through the Meteorological Assimilation Data Ingest System (MADIS, <http://madis.noaa.gov/>) which was developed by NOAA/OAR/ESRL/GSD to integrate quality control and distribute observations from NOAA and non-NOAA organizations. The Data is archived in NetCDF format files that are downloaded through the ftp site with user account and password granted by MADIS. The data availability of La Porte site is good even though there are some missing data occasionally. No long-term missing data during the study period limits the analysis. As end users for the data, we would not be in a position to validate the data. But, by comparing the observed data to model output, no suspicious sample was detected.

## 5. Results and discussions

Model result evaluations focused on model result for the TX04 domain. Statistical metric included mean (spatial-average or temporal-average), root mean square error (RMSE), mean absolute error (MAE) and bias. The formulas are listed below. Where “M” is model value, “O” is measured value and “N” is number of data points.

$$\text{Root Mean Square Error (RMSE), } E_{RMSE} = \left[ \frac{1}{N} \sum_{i=1}^N (M_i - O_i)^2 \right]^{1/2}$$

$$\text{Absolute Gross (MAE), } E_{AG} = \frac{1}{N} \sum_{i=1}^N |M_i - O_i|$$

$$\text{Bias, } B_{GB} = \frac{1}{N} \sum_{i=1}^N (M_i - O_i)$$

### *a. Identification of wind bias period*

The domain-average time series plot, including all CAMS site available in the domain, for 37 days (FIG. 3) shows the model over-predicted wind speed at peak hours (in the afternoon) and at night. In the evening hours (around 19 – 20 CST), the model wind speed increased instead of decreasing contrary to the observations. The acceleration of wind speed lasted until around midnight when the wind bias was the largest. Within this 37-day study period, the nocturnal wind bias was much less severe on certain days than others probably related to the influence of synoptic weather pattern. FIG. 4 is the spatial distribution of the wind bias at daytime and nighttime, defined as 7 – 18 CST and 19 – 6 CST next day, respectively. In coastal regions such as HGB, BEA and CCA, model overestimated the surface wind speed at most of the stations during nighttime but some stations experienced under-prediction of wind at daytime. The characteristics of wind bias problem in inland regions (DFW and ASA) are more complicated. Model tended to under-predict wind speed at daytime. But at night, both negative and positive bias can be seen in these two regions.

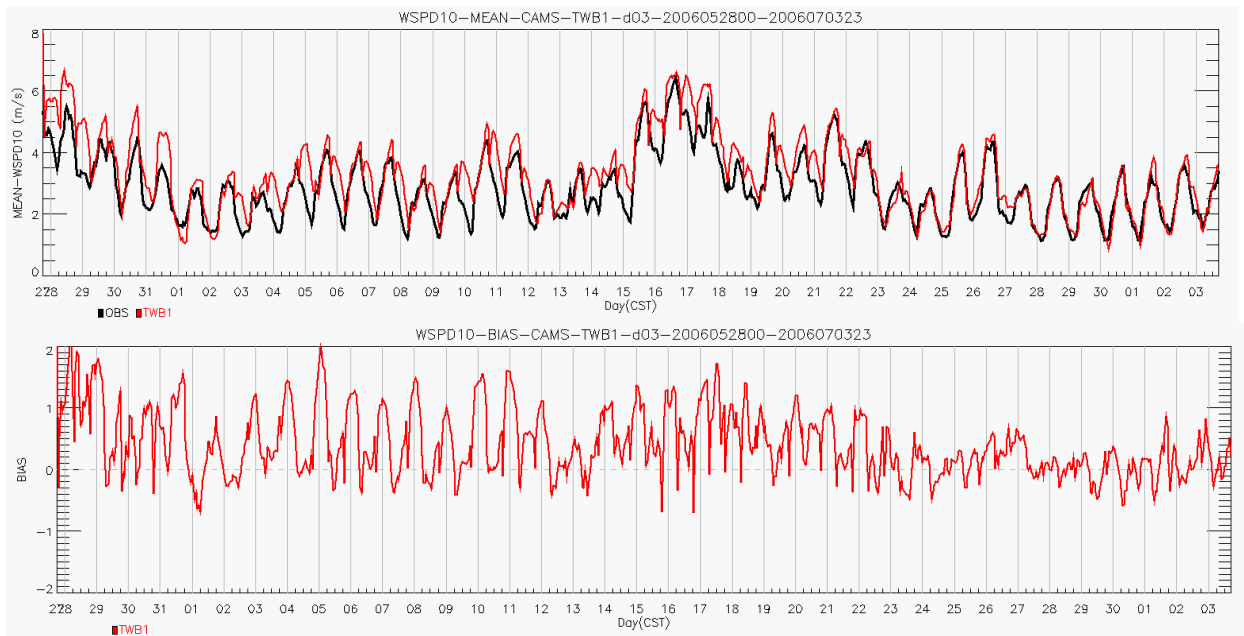


**FIG. 3** Time series of 10-m wind speed bias (model – CAMS observations) averaged for the TX04 domain. Black line is observations while red line is model result.

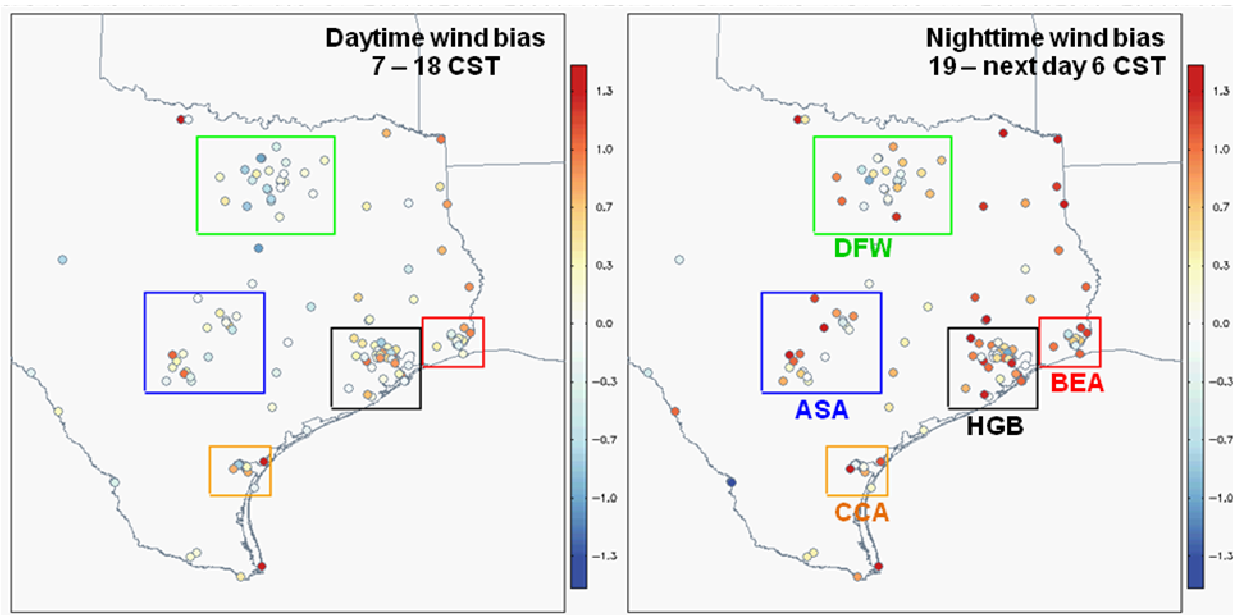
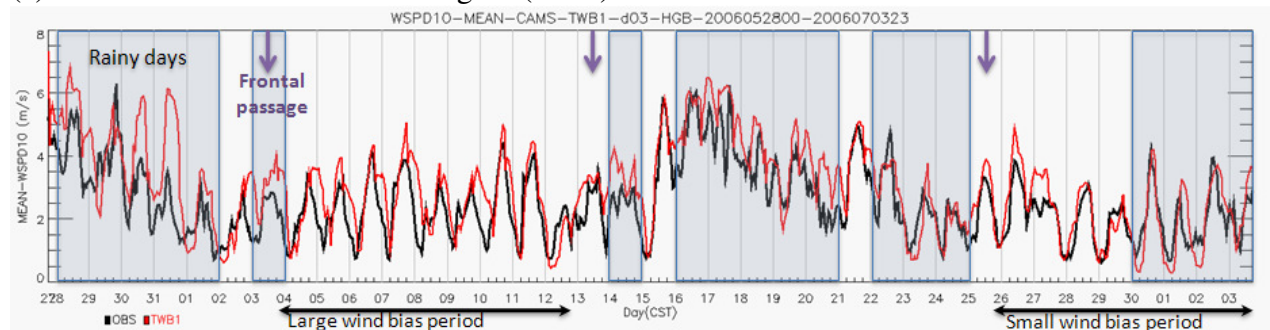


**FIG. 4** Spatial distribution of bias for 10-m wind speed for daytime hours (left) and nighttime hours (right).

Zooming in different geographically regions, FIG. 5 is time series of regional average of 10-m wind speed for HGB and DWF sectors that are considered representing coastal and inland environment respectively. Figures for the other three sectors are shown in Appendix A. Rainy days are marked as shaded area in the time series plots. We excluded these days in our analysis since the downdraft association with precipitation may lead to rapid change of wind direction and wind gust. As shown in the plots, observed wind speed varied a lot on rainy days.

There were three frontal passages in Texas during the study period – June 2/3, June 13 and June 24/25. The dates are indicated by purple arrows in FIG. 5. During the period between the first two passages of fronts i.e. 6/4 – 6/12, the evening wind bias was more severe than other days. The weather pattern over Eastern Texas was dry with high temperature (~34C in daily maximum) and no rain across the area in these 9 days. Similar to HGB, the other two coastal sectors (CCA and BEA) have the same symptoms that surface wind speed was modeled to increase at the evening hours. For inland regions (DWF and ASA), the wind bias happened occasionally but was not present daily during this period as in coastal regions. There were stormy period coming after on June 14 – 23 with frequent precipitation and various wind speed. After the frontal passage on June 24/25 (the period of 6/26 – 7/3), Southeastern Texas was subjected to cool continental air mass from the North bringing northerly to northeasterly prevailing flow to the area. The evening wind bias problem was much smaller compared to other days.

(a) Houston-Galveston-Brazoria region (HGB)



(b) Dallas-Fort Bend region (DFW)

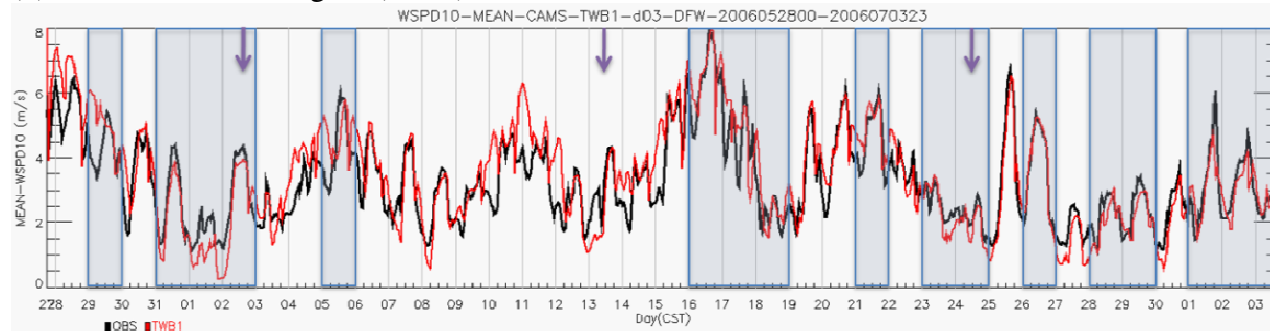


**FIG. 5 Time series of 10-m wind speed predicted by WRF (red line) and CAMS surface observations (black line) averaged for (a) HGB and (b) DFW regions. Shaded areas are rainy days and purple arrows indicate frontal passage. Black line is observations while red line is model result.**

In identifying “severe wind bias period – 6/4 to 6/12” and “less wind bias period – 6/26 to 7/3” out of the total simulation days, we computed the diurnal variation of regional average surface wind speed for these two periods as shown in FIG. 6. During the severe wind bias period (black line for observations and red line for model), the simulated wind speed dropped after the maximum wind speed in the late afternoon but increased starting at 19 CST. This symptom showed in all 5 regions and is opposing to the observed wind speed which keeps decreasing in the evening hours. Interestingly, the increase of wind speed always starts at 19 CST corresponding to sunset and the start of collapse of PBL. This may indicate the termination of solar radiation leading to the decoupling of surface cooling in the model at the sunset hour. The inaccuracy in capturing these dynamics attributed to the evening wind bias. The evening

transition hour is critical to determine the decrease of surface-driven convective mixing which is dominant in mid afternoon, and the increase of shear driven turbulence that modifies kinetic energy distribution in the lower layers and the formation of nocturnal low-level jet. In the period of 6/26 – 7/3 (grey line for observations and pink line for model), the model surface wind speed decelerated gradually during the sunset hours, in good agreement with observed values in the HGB region. Other coastal sectors show similar comparisons. However, the model still had wind bias in the inland sectors: DFW and ASA, even though the bias was not as large as those shown in coastal region during the severe wind bias period.

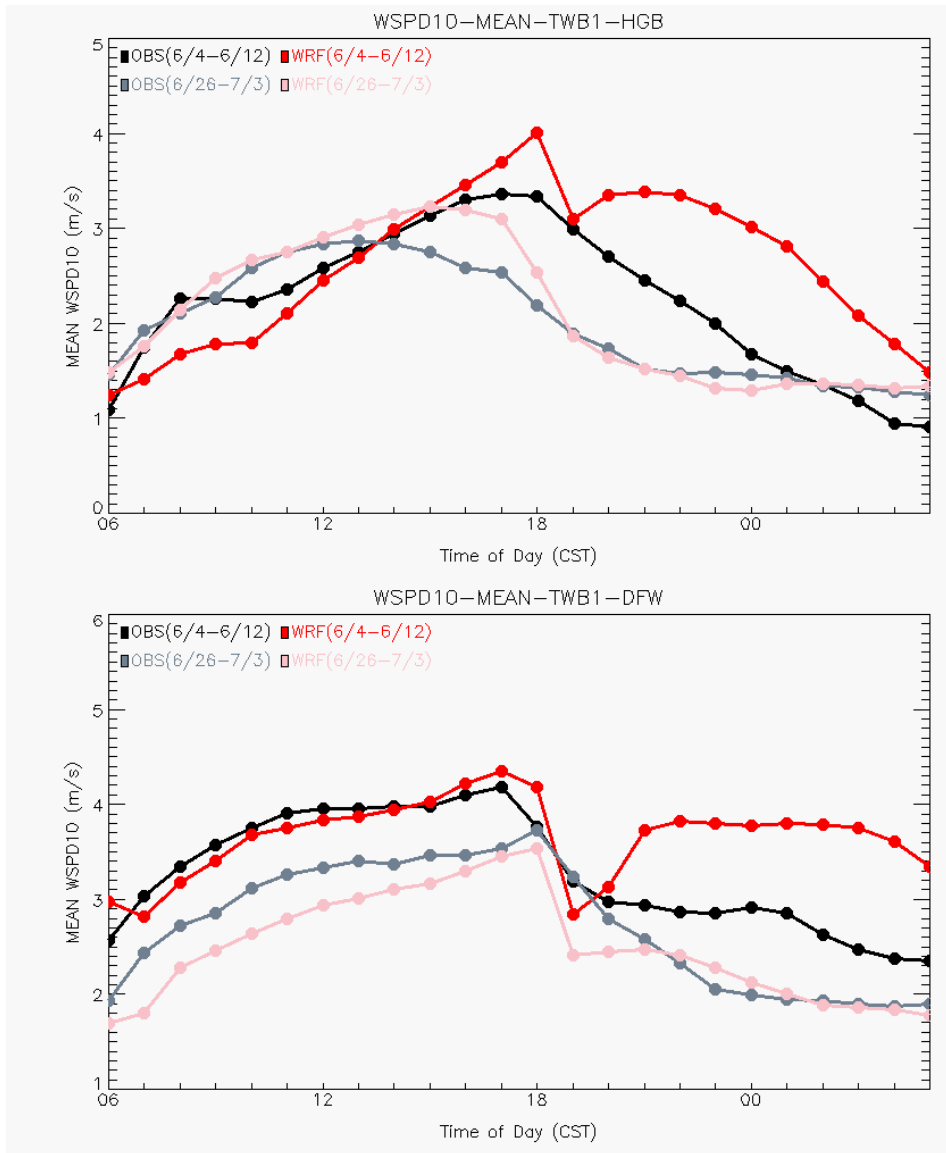


**FIG. 6** Diurnal variation of HGB (top) and DFW (bottom) regional average surface wind speed for period June 4 – 12 (dark color) and June 26 – July 3 (light color).

*b. Characteristics of weather patterns*

The composite weather charts in FIG. 7 show the distinguishable synoptic feature differences between the large wind bias and less wind bias period. A high pressure system centered at Louisiana/Mississippi/Arkansas area was present when the model repeatedly over-predicted surface wind speed in the evening hours. Southeastern Texas located at the western branch of the high pressure system experienced easterly/southeasterly synoptic wind in the low troposphere (up to 850 hPa). The local wind variation in the HGB area in the afternoon experienced this prevailing wind which was then superimposed with the sea breeze flow. Sea breeze was southeasterly/southerly penetrating the Texas coast. During the less wind bias period, a low pressure system was in control of southeast coast of the Gulf covering the HGB area with northwesterly near the surface. On the higher level (850 hPa and above), we can see a trough extended from Eastern Canada through the Northeast to Northern Texas indicating continental air mass associated with the system reaching down to the South.

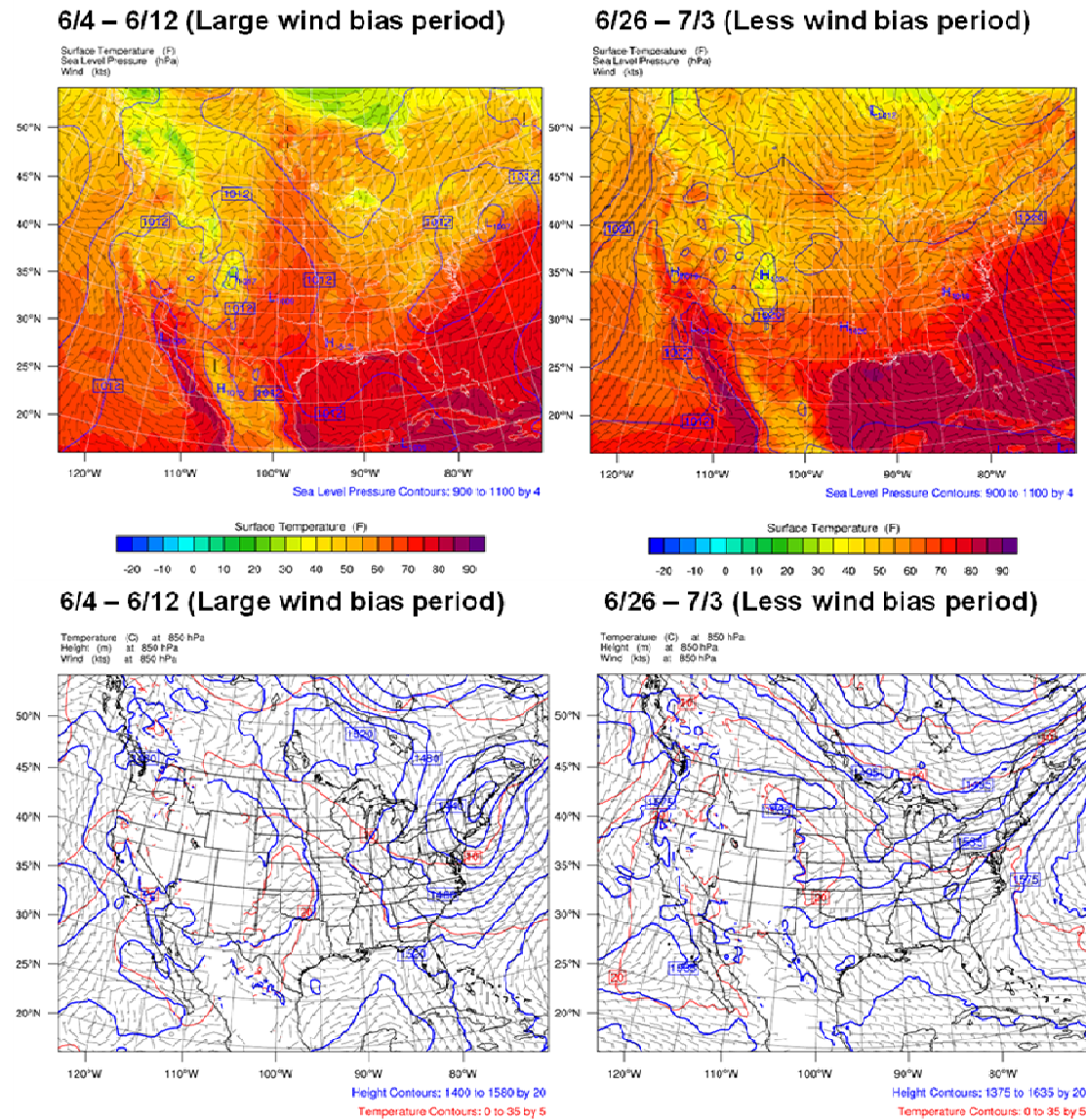


**FIG. 7** Composite weather chart for large wind bias period (6/4 – 6/12) and less wind bias period (6/26 – 7/3) at the surface (top panel) and on 850 hPa level (bottom panel).

c. Comparison at UH Coastal Center

FIG. 8 shows the time series comparison of model against the UHCC measurement for wind speed and direction. The period between 6/4 and 6/12 experienced much larger evening wind bias than other periods considered. The over-prediction of wind speed starting at the sunset hour happened repeatedly throughout the days in that period as the wind direction was dominated by southerly to southwesterly flow. However, in the period of 6/26 – 7/3, which also happened to be after frontal passage, the comparison showed much less wind speed bias. The wind direction was mainly northerly to northeasterly shifting clockwise to southerly later in the day. The 43-m height of wind measurement was compared with model at 1<sup>st</sup> and 2<sup>nd</sup> layer that are around 16.9 m and 59.4 m above ground level (FIG. 9). Both layers show similar wind biases that wind speed increases in the evening hour instead of decreases as shown in the tower observations. The diurnal cycle of 2-m temperature was well simulated (FIG. 10) despite of the nocturnal wind bias problem present or not. However, there was over-prediction of nighttime 2-m temperature in the large wind bias period. The latent heat flux has good agreement with the observations while the sensible heat flux over-predicted at daytime and under-predicted at night. Too much negative sensible heat flux and/or downward incident longwave radiative flux simulated in the model are primarily responsible for the warm bias of 2-m temperature.

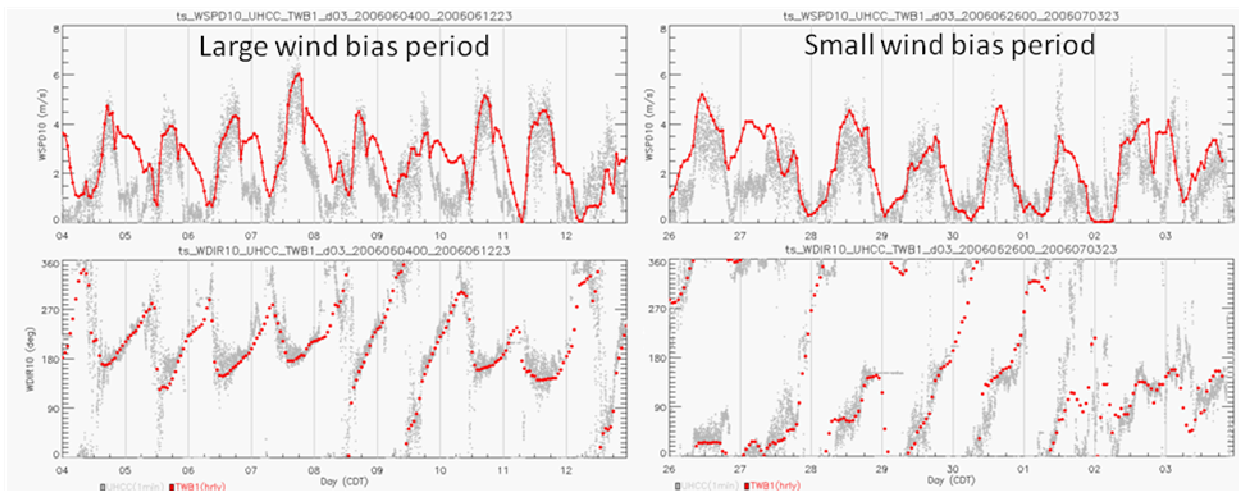
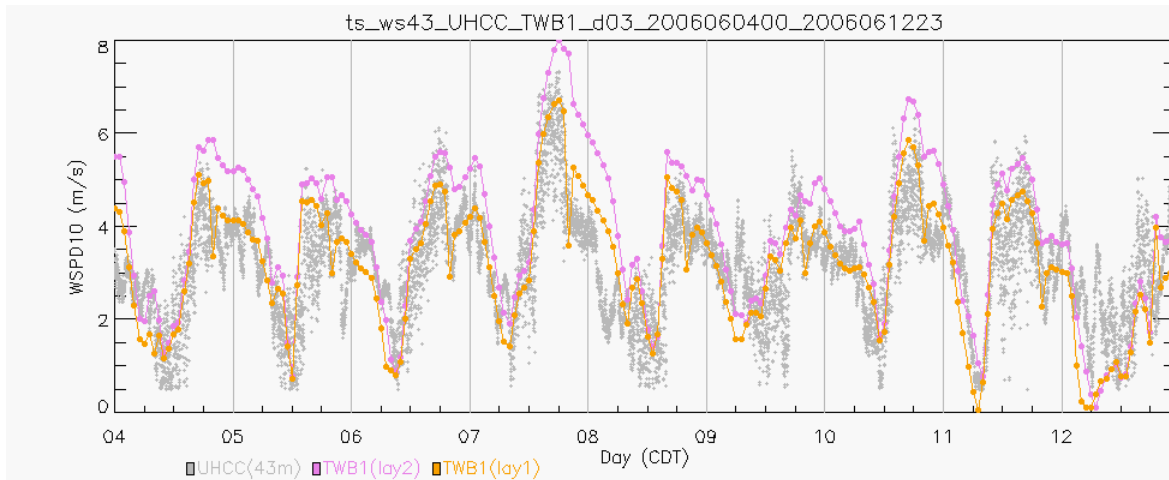
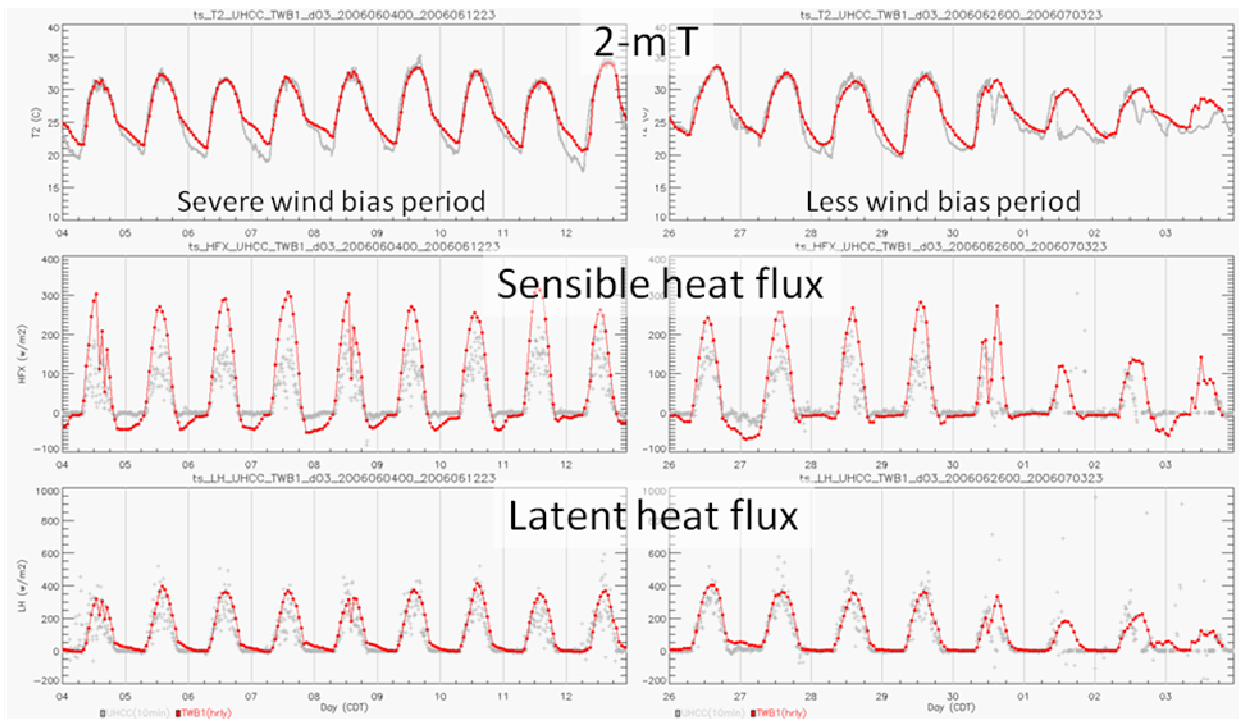


FIG. 8 Time series of 10-m wind speed (top) and wind direction (bottom) at UHCC station for large wind bias period (6/4 – 6/12, left) and small wind bias period (6/26 – 7/3, right). Gray color is observations while red color is model result.



**FIG. 9** Time series comparison of 43-m height observed wind (gray color) with 1<sup>st</sup> layer model wind (~16.9 m, pink line) and 2<sup>nd</sup> layer model wind (~59.4 m, red line) for large wind bias period at UHCC station.



**FIG. 10** Time series of 2-m temperature (top), sensible heat flux (middle) and latent heat flux (bottom) at UHCC for large wind bias period (6/4 – 6/12, left) and small wind bias period (6/26 – 7/3, right).

*d. Analysis of wind profiler paring with surface observations*

The closest CAMS station to the La Porte site is C35 whose time series of wind speed for the period 6/4 – 6/12 is shown in FIG. 11. We can clearly see the increase of wind speed at the 10-m wind and 1<sup>st</sup> layer wind in the evening. But on the 2<sup>nd</sup> layer, the model wind did not have the symptom. The nocturnal boundary layer is very shallow, typically a couple to a hundred meters or less in an urban area similar to that in the HGB region (Tucker et al. 2010). The issues of wind speed increase in the transition hour of day and night seems to be confined very close to the surface. The wind profiler site at La Porte can provide information of the wind structure vertically and temporally for the upper levels. These data will fill the gap of the tower measurement and the rest of the nocturnal boundary layer.

Both measured and model winds at the La Porte site in the lowest 3 km for June 10<sup>th</sup> and 11<sup>th</sup> are showed in FIG. 12, wind bars were color-coded with wind speed. The x-axis is the hour of day in CST while the y-axis represents altitude in km. The black line is model PBL height at the location. There was a jet core at 1.5 km height with maximum wind speed in 20 m/s and easterly wind direction. Looking at the spatial plot of model predicted wind in the upper level (See Appendix B), strong easterly flow was associated with the high pressure system centered over the areas of Louisiana, Arkansas and Mississippi. In the lower level (below 500 m), the southerly sea breeze was quite strong increasing with height and reaching maximum (10 – 15 m/s) at the top of nocturnal boundary layer. The wind turned clockwise to southwesterly as time passed throughout evening, midnight and next day early morning. There was relative lower wind speed area at around 0.7 – 1.0 km height between nocturnal low-level jet associated with the sea breeze and jet at the higher levels driven by the synoptic systems.

The wind measurement confirmed that simulated vertical structure of wind field showed a low bias in height for the jet. The model wind speed at around 0.3 and 1 km compared with the wind profiler (See Appendix C) was simulated quite well and no obvious under-prediction as mentioned in Lee et al. (2010). This indicates that the wind bias problem is confined close to the surface. The analysis for the wind profiler at Beaumont (BPATX) is not shown but reveals the similar patterns – no over-prediction of wind speed above 300 m height but strong turning of wind direction, southerly to easterly, from the surface to around 2 km height.

FIG. 13 shows the wind profiler at La Porte but for June 30<sup>th</sup> and 31<sup>st</sup> that falls in the small wind bias period in contrast with FIG. 12. During nighttime, a level-low jet was present at the height of 2.0 km which the WRF model predicted a little bit higher than the observations. Sea breeze can be seen in the afternoon with moderate wind speed. Unlike the evening wind bias case, June 30<sup>th</sup> did not get another level-low jet in the lowest 300 – 500 m above ground level. The wind speed was lowest in the surface and increased with height while wind direction was southeasterly and turned to northwesterly after midnight.

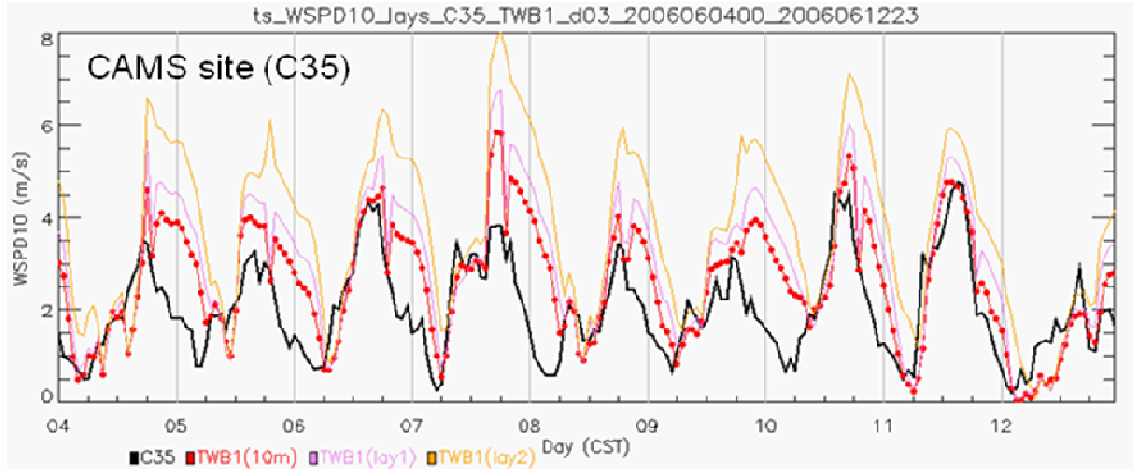


FIG. 11 Time series of wind speed of model and CAMS site C35. Observed is in black while model values are in red (10 m), pink (1<sup>st</sup> layer) and orange (2<sup>nd</sup> layer).

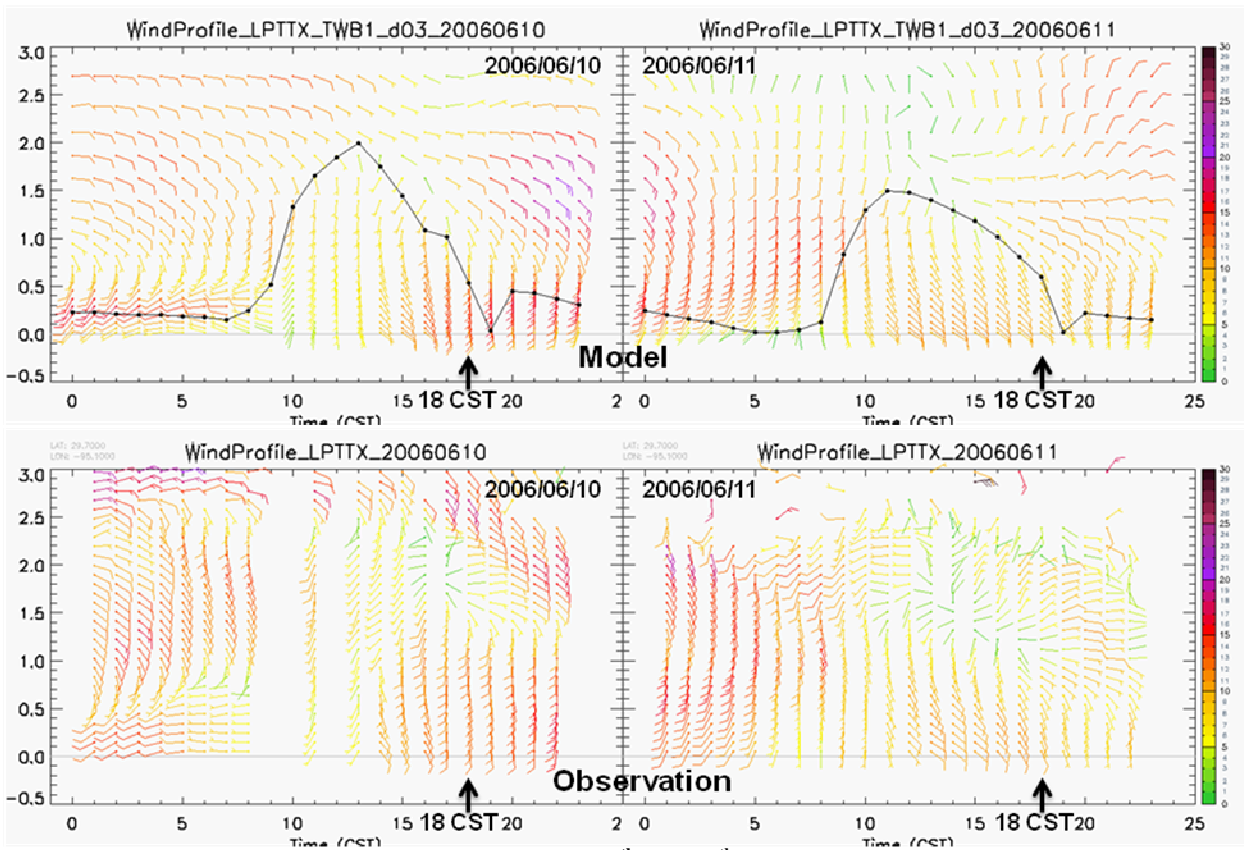


FIG. 12 Wind profiler plot at La Porte site for June 10<sup>th</sup> and 11<sup>th</sup>. Top panel: model and bottom panel: observation.

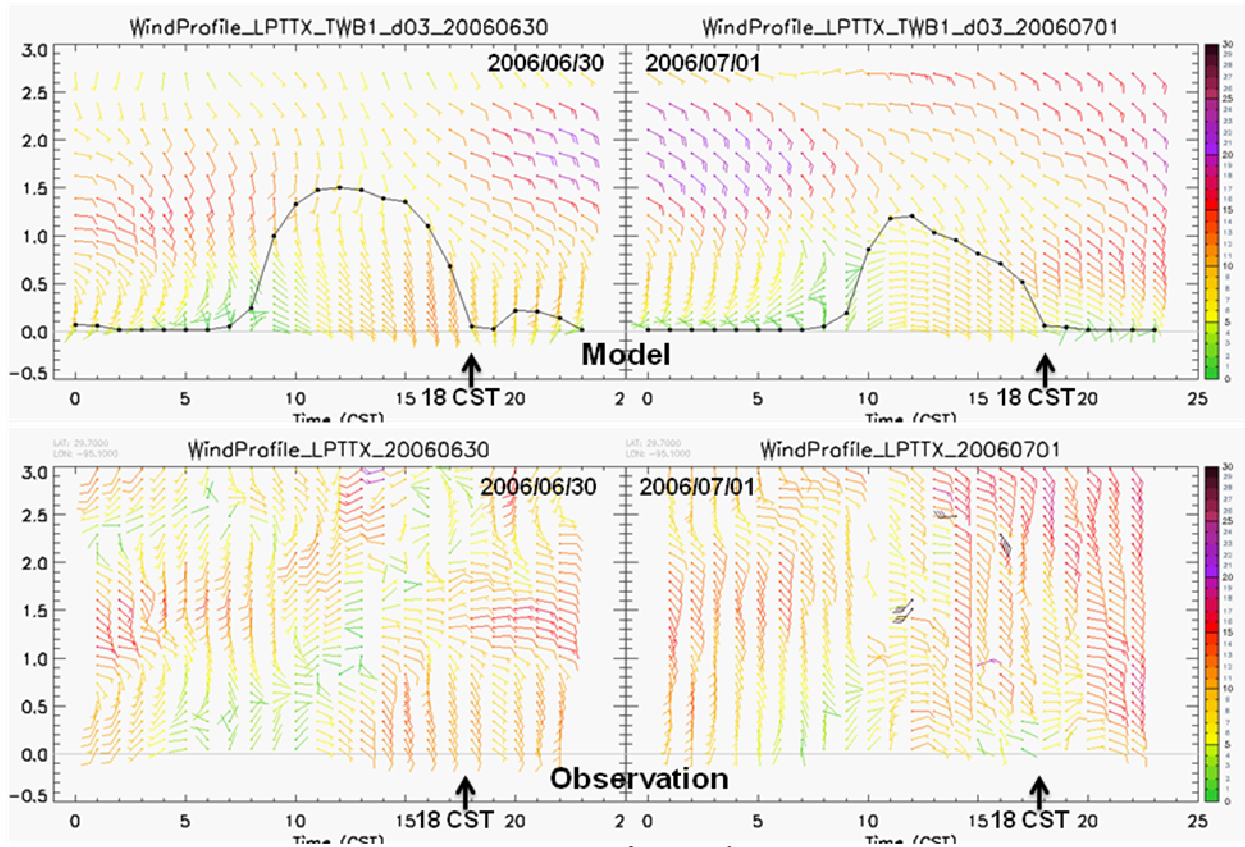
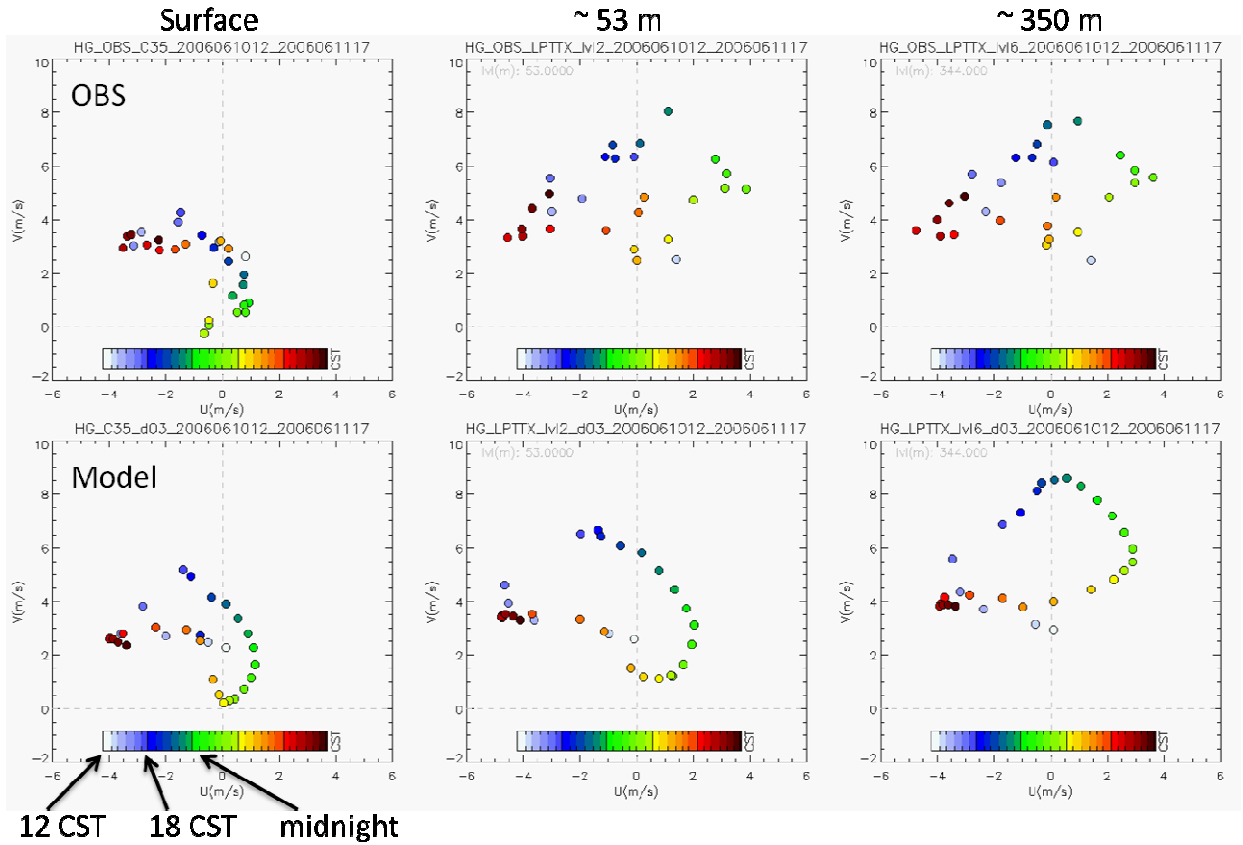


FIG. 13 Wind profiler plot at La Porte site for June 10<sup>th</sup> and 11<sup>th</sup>. Top panel: model and bottom panel: observation.

Following Van de Wiel et al 2010, we investigate the hodograph at surface and upper levels to show if model and observations experienced forward inertial oscillation in the upper level and backward inertial oscillation in the lower layer after sunset. FIG. 14 shows the hodograph on two different levels (~53 m and ~350 m) at La Porte site and surface C35 site. The dots are color-coded indicating the time of hour, starting June 10<sup>th</sup> 12 CST and ending June 11<sup>th</sup> 17 CST. The upper profiles have the nice forward turning over time in both observation and model. However, for the surface hodograph, model showed forward oscillation while observation did not. The surface hodograph at Beaumont even showed backward oscillation.



**FIG. 14** Hodograph at the surface (CAMS site C35) and La Porte site at 53m and 350m above ground level on 6/10 12 CST – 6/11 17 CST. The color of dot represents time of the hour.

## 6. Conclusive Remarks and Future Work

As wind flow is one of the critical factors affecting the accuracy of air quality modeling, the over-prediction of wind speed in the mesoscale model should be addressed seriously in the context of supporting chemical simulation, especially in air quality modeling. The nocturnal wind bias not only misplaces the ozone plume, but also jeopardizes the transport of the precursors that initiate photochemistry for the following day. In this study, we have confirmed the earlier findings by TCEQ modeling staff that the WRF-ARW model tended to increase wind speed in low levels in the Houston-Galveston-Brazoria region (HGB), at the evening hours whereas observations showed the opposite. The evening wind speed bias usually starts at around 19 CST when the sun sets resulting in the growth of nocturnal boundary layer. This is observed clearly in the coastal region such as the Houston-Galveston-Brazoria area where sea breeze is dominant in the afternoon and penetrates further inland in the evening.

During the 37-day long simulation, the period of June 4 – 12 laid between two frontal passages. It repeatedly had the wind bias problem at the sunset hours. The synoptic weather charts show a high pressure system centered at Louisiana/Mississippi/Arkansas area subjecting Southeastern Texas to have easterly/southeasterly flow in the low troposphere. The weather condition was favorable to augment sea breeze development which brings southerly to southwesterly flow to the near surface levels. In contrast, a low pressure system was in control of southeast coast of the Gulf and continental air mass reached down to the South during the small wind bias period (June 26 – July 3).

The wind tower measurement at UH Coastal Center site provides surface and near surface comparison with the model. The evening wind bias show in the 10-m wind and the 1<sup>st</sup> model layer wind (some on 2<sup>nd</sup> model layer). The wind direction was mostly southerly/southwesterly during the large wind bias period while northerly/northeasterly was dominant in the small wind bias period. Comparing the observed sensible heat flux, model was over-predicting during daytime even though 2-m temperature was well simulated. At night, too large a downward sensible heat flux was simulated resulted in a warm bias in the 2 m air temperature as indicated in the top left panel in FIG. 10.

Sea breeze induced low-level jet was present during the large wind bias period with the jet core around 300 m height. In higher levels (around 1.5 – 2km), another wind speed maximum can be seen. These two characteristics were associated with the high pressure system centered in the Southeastern states. In the less wind bias period, a similar jet core was present at the height of 1.5 – 2km. But the sea breeze was much weaker and the thickness of the southerly flow was thinner than the wind bias case. The wind turning within the nocturnal boundary layer was forward oscillation in the nocturnal boundary layer shown in both model and wind profiler. But the observed wind had counterclockwise turning in the evening hours while model 10-m wind still showed clockwise oscillation.

The theoretical work on inertia oscillation accounted for frictional effects within the nocturnal boundary layer by Van de Wiel et al. (2010). This recent work contributed considerable new insight into the possible deficiencies of WRF such as timing and rate of PBL collapse soon after sunset. During the early evening hours thermal fields and its related sensible heat and latent heat

fluxes re-establish themselves from the abrupt cutoff of intensive solar heating and similarly quick response from night time radiation cooling. The high bias in low level wind can also be due to a mismatch in timing and rate of the PBL collapse. The rapid growth of the nocturnal boundary layer from below is carving a stagnant zone in the lowest level. This layer detaches the residual layer from the surface. The WRF model does capture this evening phenomenon at around local time 19:00. Nonetheless the intricate interplay, timing and rate of such decoupling from the surface in the model may not reproduce the progression of the events, rendering the possible erroneous downward cascading of the turbulent energy within the residual layer. Frictional effect within the nocturnal boundary layer associated with inertia oscillation may have a role here. It may warrant further study to understand the parameterization of the laminar layer and its underlying similarity theory and its role in providing the frictional damping to the oscillations.

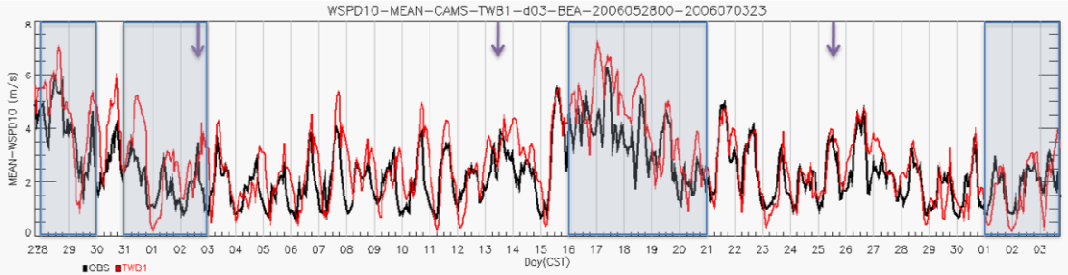
## 7. Reference

- Andreas, E. L., K. J. Claffey, and A. P. Makshtas, 2000: Low-level atmospheric jets and inversions over the Western Weddell Sea. *Bound-Layer Meteor.*, **97**, 459-486.
- Blackadar, A. K., 1957: Boundary layer wind maxima and their significance for the growth of nocturnal inversions. *Bull. Amer. Meteor. Soc.*, **38**, 283-290.
- Banta, R. M., C. J. Senff, J. Nielsen-Gammon, 429 L. S. Darby, T. B. Ryerson, R. J. Alvarez, S. P. Sandberg, E. J. Williams, and M. Trainer, 2005: A Bad Air Day in Houston. *Bull. Amer. Meteor. Soc.*, **86**, 657-669.
- Banta, R.M., Senff, C.J., Alvarez, R.J., Langford, A.O., Parrish, D.D., Trainer, M.K., Darby, L.S., Hardesty, R.M., Lambeth, B., Neuman, J.A., Angevine, W.M., Nielsen-Gammon, J., Sandberg, S.P., White, A., 2011. Dependence of daily peak O<sub>3</sub> concentrations near Houston, Texas on environmental factors: wind speed, temperature, and boundary-layer depth. *Atmos. Environ.*, **45**, 162-173.
- Byun, D.W. and S.P.S. Arya, 1986: A study of mixed layer momentum evolution. *Atmos. Environ.*, **20**, 715-728
- Byun, D. W., M. D. Jang, C. K. Song, S. T. Kim, F. Y. Cheng, R. Perna and H. C. Kim 2007: Operational Evaluation of the Eastern Texas Air Quality (ETAQ) Forecasting System Based on MM5/SMOKE/CMAQ. *Development in Environmental Science*, **6**, 253-261.
- Byun, D. W., F. Ngan, X. S. Li, D. G. Lee, S. T. Kim and H. C. Kim, 2008: Evaluation of retrospective MM5 and CMAQ simulation of TexAQS-II Period with CAMS measurements. *Final Report for Texas Commission on Environmental Quality*, February 2008, 30 pp.
- Chen, B., A. F. Stein, N. Castell, J. D. de la Rosa, A. M. de la Campa, Y. Gonzalez-Castanedo, R. R. Draxler, 2012: Modeling and surface observations of arsenic dispersion from a large Cu-smelter in southwestern Europe. *Atmos. Environ.*, **49**, 114-122.
- Dudhia, J., 1989: Numerical Study of Convection observed during the Winter Monsoon Experiment using a mesoscale two-dimensional model, *J. Atmos. Sci.*, **46**, 3077-3107.
- Gilliam, R. C. and J. E. Pleim, 2010: Performance Assessment of New Land Surface and Planetary Boundary Layer Physics in the WRF-ARW. *J. Appl. Meteor. Climatol.*, **49**, 760 - 774.
- Grell, G.A., Dudhia, J., Stauffer, D., 1994. A description of the fifth-generation Penn State/NCAR mesoscale model (MM5), *NCAR Technical Note: NCAR/TN-398pSTR*.
- Hong, S.-Y., J. Dudhia, and S.-H. Chen, 2004: A Revised Approach to Ice Microphysical Processes for the Bulk Parameterization of Clouds and Precipitation, *Mon. Wea. Rev.*, **132**, 103–120.
- Hong, S.-Y., and J.-O. J. Lim, 2006: The WRF Single-Moment 6-Class Microphysics Scheme (WSM6), *J. Korean Meteor. Soc.*, **42**, 129–151.
- Hong, S.-Y., and Y. Noh, and J. Dudhia, 2006: A new vertical diffusion package with an explicit treatment of entrainment processes. *Mon. Wea. Rev.*, **134**, 2318–2341.

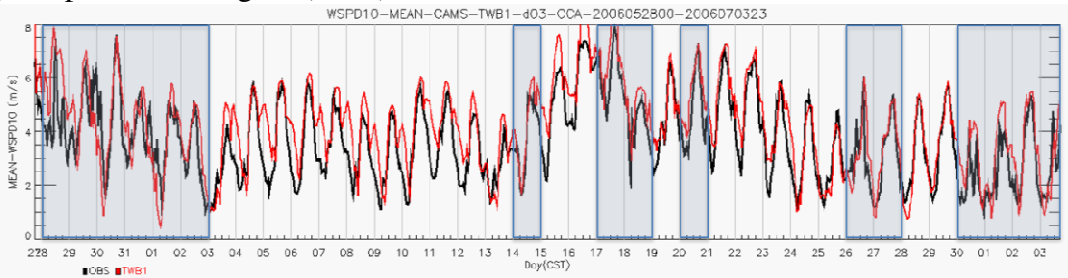
- Kain, J. S., 2004: The Kain-Fritsch convective parameterization: An update. *J. Appl. Meteor.*, **43**, 170–181.
- Lee, S. H., S. W. Kim, W. M. Angevine, L. Bianco, S. A. McKeen, C. J. Senff, M. Trainer, S. C. Tucker, and R. J. Zamora, 2010: Evaluation of urban surface parameterizations in the WRF model using measurements during the Texas Air Quality Study 2006 field campaign, *Atmos. Chem. Phys.*, **11**, 2127-2143.
- Ngan, F., D. W. Byun, H. C. Kim, D. G. Lee, B. Rappenglueck and A. Pour-Biazar, 2012: Performance assessment of retrospective meteorological inputs for use in air quality modeling during TexAQS 2006. *Atmos. Environ.*, In Press.
- Nielsen-Gammon, J., 2002: Validation of physical processes in MM5 for photochemical model input: The Houston 2000 ozone episode. 2002 MM5 Workshop, Boulder, CO, NCAR.
- Otte, T.L., 2008: The impact of nudging in the meteorological model for retrospective air quality simulations. Part I: Evaluation against National Observation Networks. *J. Appl. Meteor. Climatol.*, **47**, 1853 - 1867.
- Mlawer, E. J., S. J. Taubman, P. D. Brown, M. J. Iacono and S. A. Clough, 1997: Radiative transfer for inhomogeneous atmosphere: RTTM, a validated correlated-k model for the longwave, *J. Geophys. Res.*, **102**, 16663-16682.
- Skamarock, W. C., and Coauthors, 2008: *A description of the advanced research WRF version 3*. NCAR Tech Note NCAR/TN-475+STR, 125 pp.
- Tucker, S. C., R. M. Banta, A. O. Langford, C. J. Senff, W. A. Brewer, E. J. Williams, B. M. Lerner, H. Osthoff, and R. M. Hardesty, 2010: Relationships of coastal nocturnal boundary layer winds and turbulence to Houston ozone concentrations during TexAQS 2006, *J. Geophys. Res.*, **115**, D10304, doi:10.1029/2009JD013169.
- Van de Wiel, B. J. H., A. F. Moene, G. J. Steeneveld P. Baas, F. C. Bosveld, and A. A. M. Holtslag, 2010: A conceptual view on inertial oscillations and nocturnal low-level jets. *J. Atmos. Sci.*, **67**, 2679-2689.
- Zhang, Da-Lin, Wei-Zhong Zheng, 2004: Diurnal cycles of surface winds and temperatures as simulated by five boundary layer parameterizations. *J. Appl. Meteor.*, **43**, 157–169.

## Appendix A

### (c) Beaumont region (BEA)



### (d) Corpus Christi region (CCA)

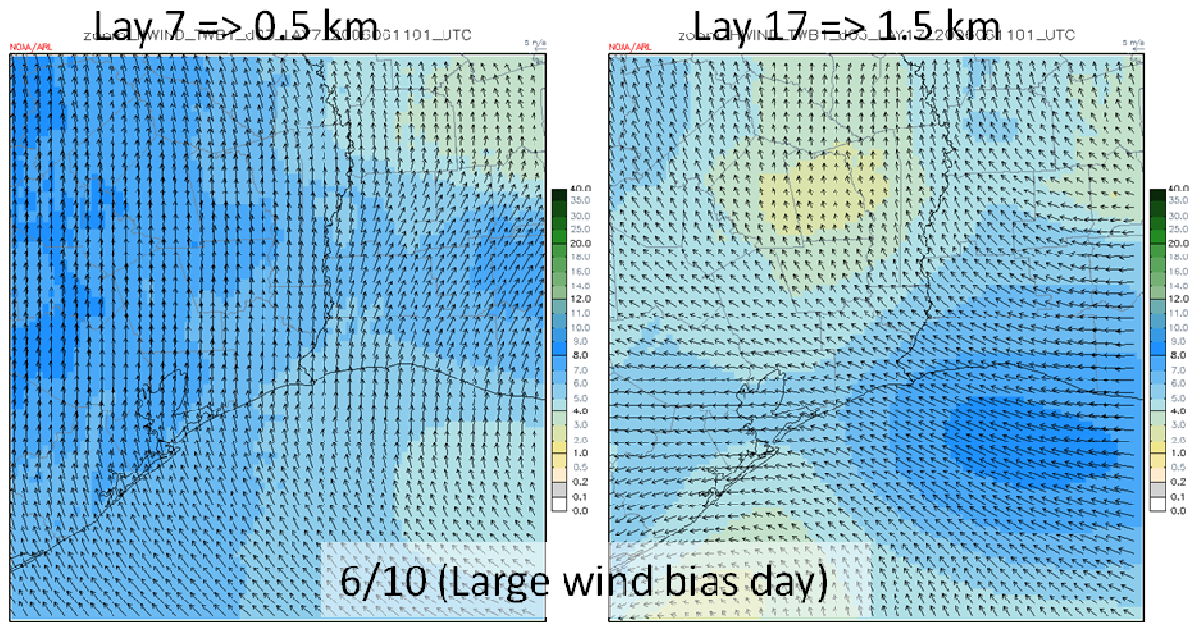


### (e) Austin-San Antonio region (ASA)



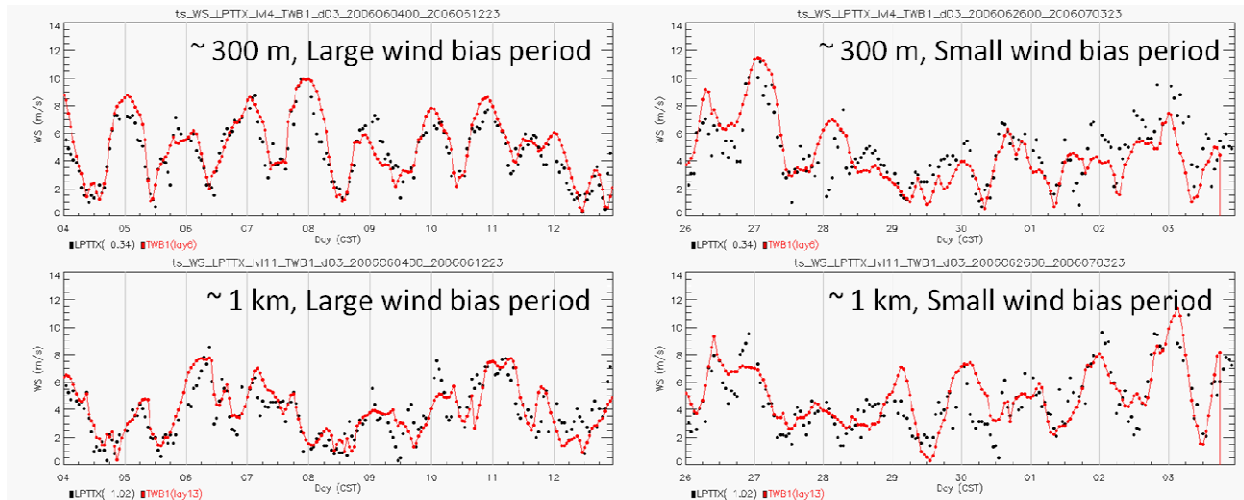
Time series of 10-m wind speed predicted by WRF (red line) and CAMS surface observations (black line) averaged for (a) BEA, (b) CCA and (c) ASA regions. Shaded areas are rainy days and purple arrows indicate frontal passage. Black line is observations while red line is model result.

## Appendix B



Spatial plots of model wind speed (shaded) and wind arrows zooming in southeastern Texas at about 500 m and 1.5 km height above ground level at 19 CST on 6/10.

## Appendix C



Time series of the observed and simulated wind speed at about 300 m and 1 km height above ground level at La Porte wind profiler site for two study periods: larger wind bias period (6/4 – 12) and small wind bias period (6/26 – 7/3).